







RESEARCH ARTICLE OPEN ACCESS

Longitudinal Changes of Quantitative Brain Tissue Properties Induced by Balance Training

Norman Aye¹  | Nico Lehmann^{1,2}  | Jörn Kaufmann³  | Hans-Jochen Heinze^{3,4,5,6} | Emrah Düzel^{4,5,7,8}  | Gabriel Ziegler^{4,7}  | Marco Taubert^{1,5} 

¹Faculty of Human Sciences, Institute III, Department of Sport Science, Otto von Guericke University, Magdeburg, Germany | ²Department of Neurology, Max Planck Institute for Human Cognitive and Brain Sciences, Leipzig, Germany | ³Department of Neurology, Otto von Guericke University, Magdeburg, Germany | ⁴German Center for Neurodegenerative Diseases (DZNE), Magdeburg, Germany | ⁵Center for Behavioral and Brain Science (CBBS), Otto von Guericke University, Magdeburg, Germany | ⁶Leibniz-Institute for Neurobiology (LIN), Magdeburg, Germany | ⁷Institute of Cognitive Neurology and Dementia Research, Otto von Guericke University, Magdeburg, Germany | ⁸Institute of Cognitive Neuroscience, University College London, London, UK

Correspondence: Norman Aye (norman.aye@ovgu.de)

Received: 22 April 2024 | **Revised:** 3 December 2024 | **Accepted:** 23 December 2024

Funding: This work was supported by Otto von Guericke University Magdeburg (2039236003) (funded to Norman Aye).

Keywords: brain microstructure | motor learning | MPM | MRI | neuroplasticity

ABSTRACT

The human brain can show remarkable experience-induced plasticity under conditions such as aging and pathology. However, the mapping of changes provided by many imaging approaches often lacks specificity with respect to biological tissue properties, which is relevant for treatment optimization and the evaluation of health-promoting lifestyle factors. Training-induced structural changes in cortical and subcortical gray matter likely reflect a mixture of various microstructural processes. In order to non-invasively map these different microstructural contributions, we used quantitative magnetic resonance imaging (qMRI) to measure clinically-relevant brain tissue property changes (such as iron, myelin, and water) in response to 4 weeks of motor balance training in 26 healthy young adults. Training resulted in a regionally-specific decrease in myelin-related magnetization transfer saturation (MT_{sat}) in the left frontal cortex. We also found performance-related changes in iron-sensitive transverse relaxation rate ($R2^*$) in visual cortical (signal increase along with positive performance correlation) and limbic subcortical (signal decrease along with negative performance correlation) brain areas. Our study contributes to a growing body of literature investigating motor training-induced microstructural brain plasticity. Specifically, we provide new insights into microstructural brain changes using whole-body motor learning (balance practice) and longitudinal quantitative mapping of brain tissue properties.

1 | Introduction

Brain plasticity is the ability of the nervous system to undergo transient or lasting functional or structural changes in response to external or internal stimuli (Konorski 1949; Paillard 1976) as well as motor skill acquisition and adaption to unexpected or novel situations (Azzarito et al. 2023; Biel et al. 2020; Draganski et al. 2004). Recent theoretical accounts of brain

plasticity often describe functional correlates and time course of training-induced structural brain changes and their respective changes across the human lifespan (Kheirbek et al. 2013; Lövdén et al. 2010; Wenger, Brozzoli et al. 2017; Wenger, Kühn et al. 2017).

In order to measure and track training-induced plasticity in vivo in the human brain, researchers have used non-invasive

Abbreviations: GM, gray matter; ICC, intra-class-correlation coefficient; k, number of raters; MT_{sat} , magnetization transfer saturation; n, number of subjects; PD, proton density; R1, longitudinal relaxation time; $R2^*$, transversal relaxation time; SD, standard deviation; WM, white matter.

This is an open access article under the terms of the [Creative Commons Attribution-NonCommercial-NoDerivs](https://creativecommons.org/licenses/by-nc-nd/4.0/) License, which permits use and distribution in any medium, provided the original work is properly cited, the use is non-commercial and no modifications or adaptations are made.

© 2025 The Author(s). *Human Brain Mapping* published by Wiley Periodicals LLC.

magnetic resonance imaging (MRI) (Green and Bavelier 2008; Surgent et al. 2019; Tymofiyeva and Gaschler 2020). Using MRI and voxel-based morphometry of T1-weighted (T1w) brain images (Ashburner and Friston 2005), morphometric changes in cortical and subcortical brain regions can be investigated, for instance, by physical exercise or learning interventions (Draganski et al. 2004; Zatorre, Fields, and Johansen-Berg 2012). Previous studies in the field showed highly dynamic and task-specific changes in local gray matter volumes in response to motor training and were able to demonstrate changes in gray matter after several weeks or months of motor training (Boyke et al. 2008; Draganski et al. 2006; Draganski et al. 2004), more recent studies found very rapid and transient plasticity in task-specific motor regions after just one or a few training sessions and thus at a very early stage of skill acquisition (Nierhaus et al. 2021; Olivo et al. 2022; Taubert et al. 2016; Wenger, Kühn et al. 2017). Such different time courses of morphometric MRI changes are difficult to reconcile with a uniform underlying cellular correlate (Song et al. 2022). The neurobiological processes driving the training-induced MRI signal changes are still difficult to address, mainly because conventional T1w MRI is not suited to quantify specific microstructural tissue processes (Tardif et al. 2016). Instead, the gray matter tissue segments derived from T1w images represent a 3D arrangement of arbitrary grayscale units that are influenced by the size, shape, and density of the underlying tissue (Lövdén et al. 2013). Morphometric training-induced GM brain changes are a result of changes in cortical thickness, tissue density, surface area, and cellular composition of tissue microstructure, or some permutation of these factors (Asan et al. 2021; Wenger, Brozzoli et al. 2017). Therefore, it is likely that changes in gray matter at different stages of motor skill learning do reflect different microstructural plasticity processes or a mixture of these. This lack of biological specificity of classical morphometric indices limits scientific progress in this field and hinders the clinical application of treatment strategies targeted at a specific pathological process. Therefore, it is critical to test the reliability and responsiveness of novel, biologically more specific MRI parameters in the context of interventions that allow the effects of behavioral training on clinically relevant brain tissue properties to be assessed.

Quantitative magnetic resonance imaging (qMRI) (Weiskopf et al. 2015) provides insight into microstructural processes. Multi-parameter mapping (MPM) is one specific qMRI method which uses multiple quantitative brain maps of improved biological specificity such as magnetization transfer saturation (MT_{sat}), proton density (PD), longitudinal relaxation time (R1), transversal relaxation time (R2*). Respectively, histological validation studies support the relationship between qMRI parameters and specific biological processes (Campbell et al. 2018; Ghadery et al. 2015; Henkelman, Stanisz, and Graham 2001; Langkammer et al. 2010; Lema et al. 2017). For example, MT_{sat} imaging is related to cortical and subcortical myelin content (Cercignani and Barker 2008; Glasser et al. 2014; Heath et al. 2018; Henkelman, Stanisz, and Graham 2001; Henkelman et al. 1993; Turati et al. 2015), R2* is mainly sensitive to iron (Barbosa et al. 2015; Langkammer et al. 2013; Langkammer et al. 2010), PD has the most sensitivity to water content in the brain (Carey et al. 2018; Fatouros et al. 1991; Fatouros and Marmarou 1999) and R1 is sensitive to either myelin (Lutti et al. 2014), water (tissue) and iron content (Gelman et al. 2001),

indicating reduced specificity of R1 compared to MT_{sat} , R2*, and PD (Georgiadis et al. 2021; Tofts 2003).

Previous plasticity and aging studies primarily employed R1 to track microstructural changes within the cortex (Matuszewski et al. 2021; Rowley et al. 2019; Shao et al. 2022; Yeatman, Wandell, and Mezer 2014). To date, only one training study has assessed changes in multiple MPM parameters concurrently (Azzarito et al. 2023), which showed specific temporal and spatial properties of microstructural changes induced by motor skill learning using a computer-based motion game. Consideration of multiple structural brain imaging indices, as also suggested in the literature (Draganski and Kherif 2013; Song et al. 2022; Tardif et al. 2016), may improve the interpretation of the neurobiological correlates underlying behavioral training. This suggests that an integrative analysis of multiple qMRI maps may offer complementary evidence for or against certain changes in microstructural tissue properties (e.g., myelin). This approach can thus provide more granular insights compared with looking at individual metrics (Draganski and Kherif 2013; Weiskopf et al. 2013).

The aim of this study is to comprehensively map microstructural gray matter changes using MPM's of R1, MT_{sat} , PD, and R2* in response to 4 weeks of training in a challenging dynamic balance task (DBT) (McNevin, Shea, and Wulf 2003; Shea and Wulf 1999). The MPM metrics offer valid and reliable (Aye et al. 2022; Leutritz et al. 2020) insights into brain tissue property changes over short periods of time (intraclass correlation coefficient as a marker for reliability [ICC] over 4 weeks in cortex and subcortex) between 0.789 and 0.264 by Aye et al. and in global voxelwise GM between 0.728 and 0.883 by Wenger et al. (2022), and a coefficient of variance between 4% and 16% (Leutritz et al. 2020). In order to relate motor training to quantitative brain tissue changes we modeled individual motor learning performance over sessions (Lehmann et al. 2023; Lehmann, Villringer, and Taubert 2022). In the context of our previous findings with the whole-body balance training paradigm (Taubert et al. 2010), we expect microstructural changes in prefrontal regions (medial frontal cortex, middle frontal cortex, and orbitofrontal cortex) and in motor-related areas (supplementary motor area), as these are present in the early and late learning phases of this task. Using qMRI data acquired pre and post-training, we, therefore, tested for training-related voxel-wise microstructural brain changes (1) in prefrontal and motor-related brain regions (a priori regions-of-interest) and (2) across the whole cortex and subcortical regions in an exploratory analysis approach.

2 | Material and Methods

2.1 | Participants and Experimental Design

To assess microstructural changes through dynamic whole-body balance training (DBT) we acquired three MRI scans with a scan-to-scan interval of 4 weeks in between (first period was the control period (interval between MRI-1 and MRI-2), second period was the intervention period (interval between MRI-2 and MRI-3); Figure 1A) which is strong controlled within-subjects test design referred to Thomas and Baker (2013). None of the 26 healthy participants (4 ♀, 22 ♂; age: mean = 22.1, SD = 3,

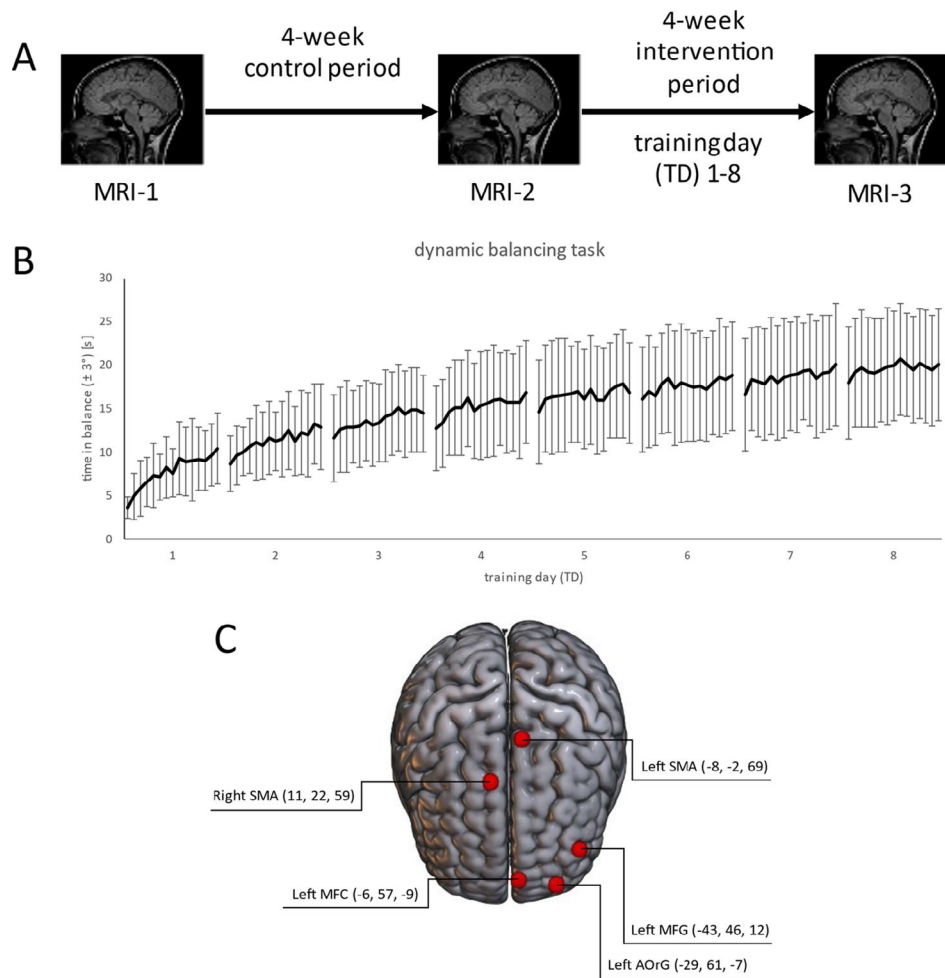


FIGURE 1 | (A) Overview of the control and training period of the study. In each MRI session, we used the same measurement protocol for the multi-parameter maps (MPM's) based on Weiskopf et al. (2013). (B) Average performance (time in balance ± 1 SD) of each DBT trial of the $n = 26$ participants during the 4-week intervention period. (C) ROIs with structural changes in gray matter in the late DBT learning phase, based on the previous study by Taubert et al. (2010). ROIs (red dots) are superimposed on a rendered template in MNI152 space. MNI coordinates and anatomical labels (according to the Neuromorphometrics atlas) are listed next to the ROIs.

range 19–29; BMI: mean = 21.2, SD = 2.3, range 17.6–25.6) had a history of systemic, psychiatric or neurological diseases. We excluded participants with high expertise in balance-focused sports like dancing or horse riding or with previous experience with the task to be learned (DBT). Further exclusion criteria were body mass index (BMI) $> 30 \text{ kg/cm}^2$, contraindications to MRI, left-handedness, and self-reported vigorous physical activity $> 4 \text{ h}$ per week. Participants were instructed to avoid any balance-specific or coordinative-demanding sports throughout the intervention and control periods. This study sample was a subset of subjects that participated in our previous reliability studies (Aye et al. 2022; Lehmann et al. 2021). The study was carried out in accordance with the Declaration of Helsinki and approved by the Ethics Committee of the Otto von Guericke University Magdeburg (approval number 106/98). Written informed consent was obtained from all participants.

2.2 | Dynamic Whole Body Balancing Task

After the second MRI scan (MRI-2, see Figure 1), the participants received 8 training sessions of the DBT on a

seesaw-like platform (stability platform, model 16,030, Lafayette Instruments, Lafayette, IN). The balance platform has a maximum deviation of $\pm 26^\circ$ on each side and is moveable in the mediolateral direction. Within the intervention period of 4 weeks, each participant completed two DBT training sessions per week with at least 24 h between sessions. Each training session contained 15 training trials with a duration of 30 s each (Figure 1B), and participants were given a 2-min rest period between trials to avoid muscle fatigue.

Participants were instructed to keep the balance platform within a deviation range of $\pm 3^\circ$ from the horizontal for as long as possible during each trial (Taubert et al. 2010), while focusing their attention on a cross on the wall directly in front of them (placed directly in the line of sight). The behavioral outcome measure was the “time in balance” (in seconds), which is defined as the cumulated time spent within the aforementioned deviation range during each 30-s trial. After each trial, the participants received verbal feedback about their time in balance (knowledge of results) while no further information about the optimal movement strategy was provided (discovery-learning strategy, Orrell, Eves, and Masters 2006).

We used the repeated measurement (RM) ANOVA for quantifying the performance improvements for all training sessions including all trials.

2.3 | MRI Image Acquisition/Processing

The MRI data were acquired on a 3 T MAGNETOM Prisma system (Siemens Healthcare, Erlangen, Germany) using a 64-channel head coil. We used the same measurement protocol for each of the 26 volunteers on each of the three scanning sessions as described in Aye et al. (2022) and measured each subject at three time points with 4 weeks intervals at the same time of day whenever possible to minimize the influence of diurnal variability (Trefler et al. 2016). The time interval without training (i.e., between MRI-1 and MRI-2; see Figure 1A) served as a control period against which changes in the qMRI parameter maps occurring during training (i.e., between MRI-1 and MRI-3 as well as MRI-2 and MRI-3) were compared. All participants were instructed not to consume coffee or energy drinks directly before the measurements and not to consume alcohol 24 h before the measurements. To minimize within- and between-subject variations in head positioning, the subjects were carefully positioned in the MRI scanner by an experienced assistant medical technician. The receive head coil was fixed on the table at the same position using a hold-down groove. All subjects lay down in a supine position (head first) and landmarks were positioned between the eyebrows. The body of the participant was adjusted parallel to the B0 field before the measurement. Participants were instructed to relax and keep their minds free of any thoughts while moving as little as possible.

We acquired the MPM protocol (see e.g., Tabelow et al. 2019) using three different predominant T1-, PD-, and MT-weighted images with multi-echo FLASH scans by appropriate choice of the repetition time (TR) and the flip angle α : $TR/\alpha = 23.0 \text{ ms}/25^\circ$ for T1w scan, $23.0 \text{ ms}/5^\circ$ for PDw scan, and $37.0 \text{ ms}/7^\circ$ for MTw scan. Multiple gradient echoes were acquired with alternating readout polarity at 8 equidistant echo times (TE) between 2.46 and 19.68 ms for T1w and PDw acquisitions and at six equidistant TE between 2.46 and 14.76 ms for MTw acquisition. Other acquisition parameters were: 0.8 mm isotropic resolution, 224 sagittal partitions, field of view (FOV) = $230 \times 230 \text{ mm}$. The total acquisition time was 34.23 min. For optimizing the flip angles of the acquisitions we were using a semi-empirical approach in order to maximize signal-to-noise ratio (SNR) while limiting bias due to imperfect RF spoiling (Helms et al. 2011). The excitation flip angles for the T1- and PD-weighted gradient echo sequences were selected based on the recommendations by Helms, Dathe, and Dechent (2010), where noise propagation into the maps is minimized by choosing flip angles proportional to the Ernst angle for brain tissue, scaled by factors of 0.4142 and 2.4142, respectively. However, as highlighted by Helms et al. (2011) and supported by our practical experience, the effects of refocused transverse coherences become significant at higher flip angles. To mitigate these effects, the T1w flip angle was empirically reduced to 25° . For further details on this optimization process, we refer to Leutritz et al. (2020). Transmit and receive field correction acquisition was done prior every weighted image series (56 sagittal partitions), field

of view FOV = $230 \times 230 \text{ mm}$, TR = 4.1 ms, TE = 1.98 ms for B1- and TR = 2000 ms, TE1 = TE2 = 14 ms, 24 sagittal slices, slice thickness = 5 mm, FA = 90° , 120° , 60° , 135° , 45° for the rf map which was used for the B1+ correction as a part of the hMRI toolbox (Lutti et al. 2012; Lutti et al. 2010).

The generation of the quantitative maps was performed using the hMRI toolbox (version 0.2.0, www.hmri.info, Tabelow et al. 2019) with the recommended parameter settings as described by Aye et al. (2022). The toolbox generates (quantitative) maps of magnetization saturation (MT_{sat}), proton density (PD), longitudinal relaxation rate (R1) and transverse relaxation rate ($R2^*$).

These maps were reoriented toward a standard pose by setting the anterior commissure at the origin and both anterior and posterior commissure (AC/PC) in the same axial plane. This is a common step to increase the consistency in individual head positions prior to normalization and/or segmentation (Mazziotta et al. 2001b; Mazziotta et al. 2001a; Mazziotta et al. 1995). SPM's segmentation for example is sensitive to the initial orientation of the images (Ashburner and Friston 2005), which is addressed by this step. Note, that the header information of every reoriented image was changed without reslicing. The output resolution of processed multi-parameter maps was set to 1 mm isotropic.

2.4 | Voxel-Based Quantification (VBQ)

We used the hMRI toolbox (version 0.6.0) default settings for MT_{sat} , PD, R1, and $R2^*$ image processing. In the first step of spatial processing, we segmented the MT_{sat} images into different tissue classes (Gray matter—GM, White matter—WM, Cerebrospinal fluid—CSF) based on a probabilistic approach taking advantage of prior tissue probability maps (TPM) specifically developed for MPM's (denoted as eTPM), which has shown to result in improved segmentation (Lorio et al. 2014; Tabelow et al. 2019). Furthermore, MT_{sat} -based segmentation leads to improved subcortical contrast compared to T1w scans because of the improved delineation of white matter (WM) laminae embedded in GM structures (Helms et al. 2009). Second, we normalized individual native space images to MNI space by generating an average shaped template using DARTEL nonlinear spatial registration (Ashburner 2007). All segmented maps and GM tissues were registered to MNI space by applying the obtained deformation fields from Dartel followed by an affine transform. In the last step of spatial preprocessing, we applied tissue weighted smoothing to each map to account for potential registration inaccuracies. We used a 4 mm smoothing kernel for MT_{sat} , PD, and R1 maps, and 8 mm for $R2^*$ maps, because these settings have shown to result in optimized reliability results (Aye et al. 2022). This technique, specifically developed for qMRI (Draganski et al. 2011), allows us to improve spatial realignment by preserving quantitative values within tissue classes (not smoothing across tissue boundaries) while also accounting for partial volume contribution. Tissue weighted smoothing of MPM's according to the toolbox default settings uses individual 95% tissue probability masks (Draganski et al. 2011; Tabelow et al. 2019). The binary mask used for the subsequent statistical analyses of subcortical areas in MNI space was thresholded to a gray matter probability of 20%.

2.5 | Gray Matter Based Spatial Statistics (GBSS)

Changes in cortical gray matter were analyzed using a modified gray matter based spatial statistics (GBSS) pipeline inspired by TBSS (Nazeri et al. 2015, bash scripts available at <https://github.com/arash-n/GBSS>). In brief, GBSS uses a skeleton-based registration approach inspired by Tract-Based Spatial Statistics (Smith et al. 2006), but optimized for the conditions of the gray matter (GM). The underlying idea is to project qMRI maps to an alignment-invariant sample-specific skeleton which represents the maximally probable GM voxels (Nazeri et al. 2015), thus minimizing the potential influence of partial-volume contamination using unsmoothed images. The generation of the group-specific GM skeleton in MNI152 space based on diffusion imaging data was conducted as described in Lehmann et al. (2023). To this end, qMRI maps of each subject and measurement point were linearly registered to the respective native diffusion space, and afterwards the precomputed transformation matrices to MNI152 space were applied (Lehmann et al. 2023). Regarding the skeleton, only voxels with a GM probability of 0.5 in 50% of the subjects of the sample were retained.

3 | Statistical Analysis

3.1 | Statistical Analysis of Behavioral Data

We calculated behavioral indices for participants' initial level of performance and rate of improvement during the training period (Adams 1987; Fox, Hershberger, and Bouchard 1996). Theoretically, both initial performance and learning rate could be influenced differently by structural brain properties (Della-Maggiore et al. 2009; Sampaio-Baptista et al. 2014).

To determine DBT learning rates, we first averaged each participant's trial-wise performance values per training session (15 trials). Learning rates (exponent) and initial performance levels (base) were calculated by fitting each participant's behavioral data (8 values) with a power function, as was done by others (Lehmann et al. 2023; Lehmann, Villringer, and Taubert 2020). To correct for baseline differences, we calculated residuals of the slope values linearly corrected for the base.

3.2 | Region Based Approach

Previous training studies investigated volumetric brain changes and brain-behavioral correlations after six training sessions (one session per week) in the same complex whole-body balancing task ("Stabilometer") and identified performance-related brain changes in prefrontal and motor-related areas (Taubert et al. 2011; Taubert et al. 2010). In the present study, cumulative training-induced microstructural changes are analyzed over a longer period of time, that is, after eight training sessions dispersed over 4 consecutive weeks (two training sessions per week instead of one training session per week over 6 weeks). We predict changes in those prefrontal regions that showed plasticity in the late learning phase in the study of Taubert et al. (2010). Following a recent report of diffusion-based microstructural changes in motor-related areas in the

same sample (Lehmann et al. 2023), we will also test for MPM changes in supplementary motor areas. The region-of-interest (ROI) approach uses spheres of 5 mm radius around the coordinates of the peak voxel of each cluster. Within each of the five ROI's listed in the following (peak voxel in MNI space, see Figure 1C), we extracted the mean voxel intensities of each subject and measurement point: left medial frontal cortex (left MFC; -6, 57, -9), left middle frontal gyrus (left MFG; -43, 46, 12), left anterior orbitofrontal gyrus (left AOrG; -29, 61, -7) left and right supplementary motor area (Left SMA; -8, -2, 69; Right SMA; 11, 22, 59). We choose this sphere radius to avoid overlaps with tissue boundaries or partial volume effects (Pizzagalli et al. 2020; Wonderlick et al. 2009). The first two MRI time points (MRI-1-MRI-2; see Figure 1) were used as a control period for the observed brain changes during the intervention period (MRI-2-MRI-3). Building on prior research (Callaghan et al. 2015; Carey et al. 2018; Carter et al. 2022; Weiskopf et al. 2013), we posit that the four MPMs exhibit shared variance owing to their overlapping sensitivity to specific biological properties (Carter et al. 2022; Edwards et al. 2018). For instance, it has been reported that PD and R1 share 42% of variance due to their mutual sensitivities to water content, while MT_{sat} and R1 share 48% of variance, potentially reflecting a common sensitivity to myelin content (Carter et al. 2022). First, we conducted repeated-measures MANOVAs with MPM as the dependent variable (4 levels: R1, PD, R2*, MT_{sat}) and factors ROI (MFG, MFC, AOrG, left and right SMA) and TIME (3 levels: MRI-1, MRI-2, MRI-3; see Figure 1) to assess microstructural changes over time. Second, we performed follow-up ANOVAs within each ROI for every MPM. Finally, paired t-tests (control interval [MRI1 vs. MRI2] and intervention interval [MRI2 vs. MRI3]) using the mean value inside each MPM were carried out in each ROI (using SPSS Statistics version 25, RRID:SCR007037) and MPM changes in each ROI were correlated with motor learning rates to evaluate behaviorally related changes. We assessed the brain imaging data for normality Kolmogorow-Smirnow and found that 58 out of 60 measures were normally distributed. Additionally, we visually inspected the Q-Q plots and observed no violations of normality. Although normality violations are generally not problematic for the methods employed (Finch 2005; Knief and Forstmeier 2021), we have checked for influential outliers and deviations in the data. All results were considered significant at $p < 0.05$ for the follow-up tests.

3.3 | Exploratory Whole-Brain Analysis of Structural Changes With Behavioral Improvements

In order to explore learning-related changes in MPM microstructural maps both in the whole cortex and sub-cortical gray matter, we used the Permutation Analysis of Linear Models toolbox (PALM v. alpha119, RRID:SCR017029) (Winkler et al. 2016; Winkler et al. 2014) running in MATLAB 2020b (MATLAB, RRID:SCR001622) environment. Adopting the procedure of Lehmann et al. (2023), we are testing the complex hypothesis that the microstructural changes in the brain are indeed due to training and are behaviourally relevant. If the complex hypothesis is true, there should be evidence of neuroplastic change in the time intervals MRI1_MRI3 and MRI2_MRI3 (as assessed

by *t*-tests against zero), and likewise, there should be evidence of correlated change between brain and learning rate in these time intervals (as assessed by linear regressions). In the absence of a traditional control group (see Thomas and Baker 2013), this procedure can largely rule out spurious results due to measurement error (especially pertaining to the time interval MRI1_MRI2) are misinterpreted as neuroplastic change. Likewise, it is important that only the incorporation of the MRI1_MRI3 time interval in the NPC allows to mitigate the potential impacts of development and/or repeated testing effects (Lehmann et al. 2023).

The four submodels (two *t*-tests, two regressions) per imaging modality were jointly tested within the modified nonparametric combination (NPC) framework (Winkler et al. 2016). NPC started by analyzing the submodels separately using synchronized permutations, therefore implicitly accounting for the non-independence between partial tests under the null hypothesis (Winkler et al. 2016). To produce a joint statistic summarizing the statistical evidence for the complex theory, the results from the submodels were then aggregated using Fisher's (1933) combining function. We used directional (one-sided) contrasts based on anticipated patterns of results (e.g., increase in microstructure and positive correlation with performance or vice versa).

For implementing the NPC analysis in the subcortex, percentage change images (MRI1_MRI3 and MRI2_MRI3) were calculated inside a 20% gray matter probability mask, and voxel-wise PALM-based NPC analysis was spatially restricted to this mask (voxel-based quantification, VBQ). Analysis in cortical GM areas was conducted using GBSS (see above), which means that the microstructure maps projected onto the group-specific gray matter skeleton were used. Percentage change images were also calculated here, which were then analyzed within a mask of the gray matter skeleton (Nazeri et al. 2015). Note that only 24 subjects were included in the GBSS analysis because two participants did not have complete diffusion MRI data for all three measurement points.

For both subcortical (VBQ) and cortical (GBSS) PALM-based NPC analyses, we applied threshold-free cluster enhancement (TFCE; Smith and Nichols 2009) to enhance cluster-like structures in the statistical images. We generated 10,000 permutations for each partial test to create an empirical null distribution, which was then used for statistical inference. The TFCE output maps underwent cluster-based family-wise error (FWE) correction using the distribution of the maximum statistic (Smith and Nichols 2009; Winkler et al. 2014). Significant results were defined at $p < 0.05$ (FWE-corrected), while potential statistical trends were evaluated at a more liberal threshold of $p < 0.1$ (FWE-corrected).

4 | Results

4.1 | Behavioral Results

Figure 1B shows the average balance performance (time in balance) across participants for each trial during the eight training sessions. We found a significant increase in balance performance over time ($F(7, 98) = 586.827$, $p \leq 0.001$, $\eta_p^2 = 0.977$).

4.2 | Region of Interest Analysis

The repeated-measurement MANOVA for all ROIs and all MPMs showed a significant main effect of TIME ($F(8, 18) = 3.194$, $p = 0.019$), no interaction effects between TIME and REGIONS ($F(16, 10) = 1.671$, $p = 0.207$) but a significant main effect of REGIONS ($F(8, 18) = 40.048$, $p < 0.001$). The post hoc repeated measurement ANOVA of all four MPMs in each ROI showed a significant main effect of TIME in the left MFC in MT_{sat} ($F(2, 50) = 3.379$, $p = 0.042$), in MFG in R1 ($F(2, 50) = 6.547$, $p = 0.003$) and in AOrG in MT_{sat} ($F(2, 50) = 11.889$, $p < 0.001$). We did not observe any significant changes in the left or right SMA. In the control period, we observed no significant changes in all four MPMs in the MFC and MFG, while in the left AOrG significant MT_{sat} decrease were observed ($t(25) = 3.297$, $p = 0.003$, $n = 26$). In the training period, we found a significant R1 increase in the left MFG ($t(25) = -2.159$, $p = 0.041$, $n = 26$), MT_{sat} decrease in the left MFC ($t(25) = 2.560$, $p = 0.017$, $n = 26$) but no changes in the AOrG. Direct comparisons between MPM changes in the control versus intervention periods, however, revealed no significant differences in all spheres (Table S1). Changes in PD and R1 in the MFC were highly negatively correlated ($r = -0.798$, $p < 0.001$, $n = 26$, see Figure S2), while we saw no correlation between the other MPM's. We also correlated the changes in the MPMs with the learning rate but found no significant effects on the ROIs. MPM values for all time points and ROIs are shown in Figure S1.

4.3 | Whole Brain Analysis With Brain–Behavior Correlations

Apart from changes in pre-specified ROIs, we conducted voxel-wise whole-brain analyses to explore the effects of training on the whole cortex and sub-cortex. Specifically, using the modified NPC framework, we tested for behaviorally relevant plasticity separately in the four MPM parameter maps.

With respect to subcortical analyses, we observed a non-significant trend toward a training-related decrease in $R2^*$ in the left hippocampus (left HC) that was at the same time negatively associated with a steeper learning curve ($p = 0.055$, 29 voxel for 0.061 thresholds, $n = 26$, Figure 3A,B).

Within the cortex, we found a significant increase in $R2^*$ in the right fusiform gyrus along with a positive correlation with learning rate in the DBT ($p = 0.041$, 21 voxel, $n = 24$; Figure 4). In the identified region, learning rate correlated with $R2^*$ changes between MRI-1 and MRI-3 ($r = 0.696$, $n = 24$) and MRI-2 and MRI-3 ($r = 0.349$, $n = 24$) (Figure 4B). No other learning-related MPM changes were observed in subcortical and cortical gray matter regions.

5 | Discussion

This longitudinal multi-parameter MRI study provides novel evidence for learning-related microstructural changes after 4 weeks of dynamic balance training. Microstructural changes were identified using a quantitative MPM approach that contributes

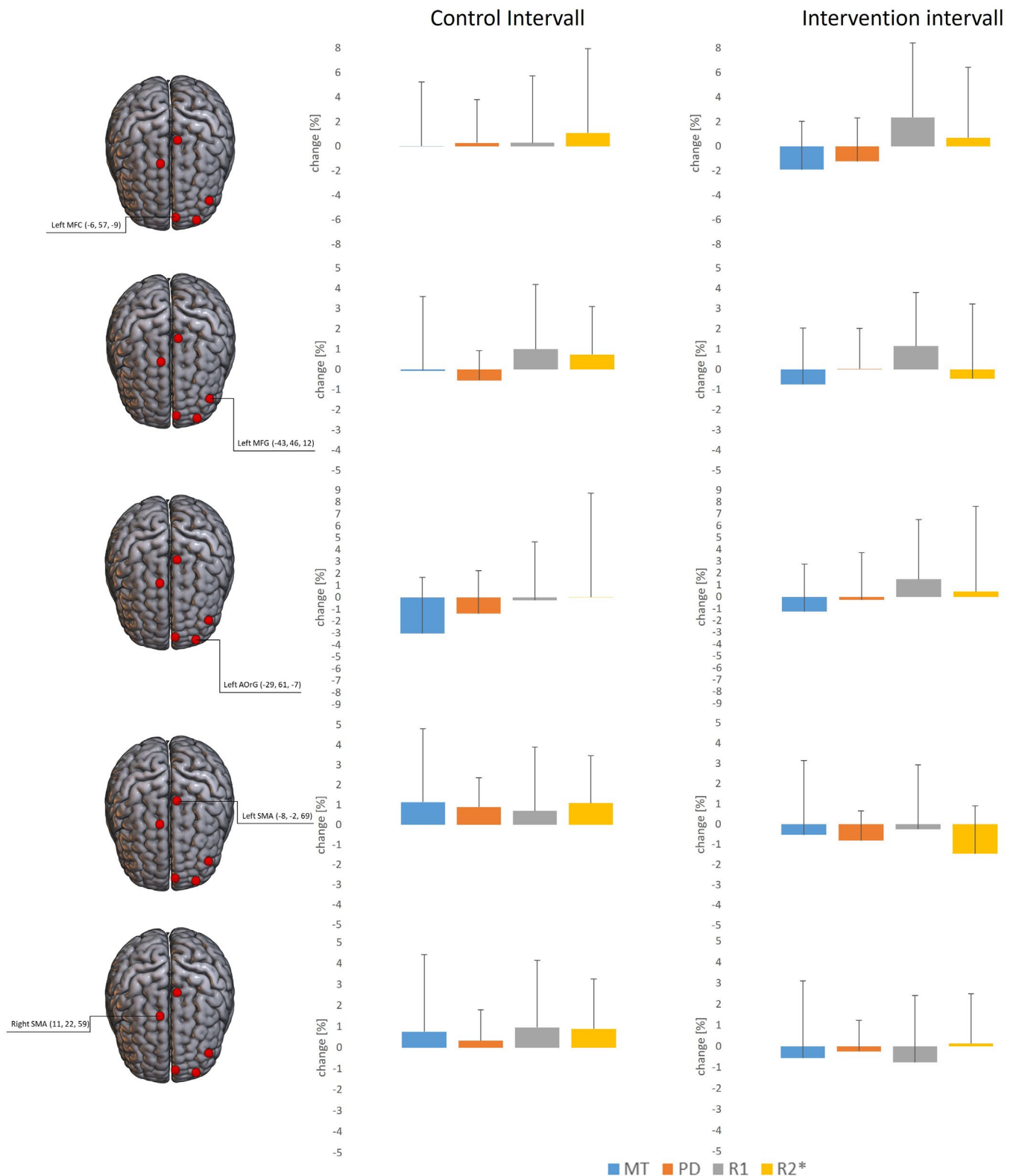


FIGURE 2 | Average percentage change and associated standard deviation in four microstructural maps (MT_{sat}: Blue, PD: Orange, R1: Gray, R2*: Yellow) in the ROIs during the control and learning phases of the experiment. Note that the indexing of the values as percentage change is for visualization purposes only, whereas in the text presented values are calculated based on dependent samples *t*-tests.

advanced information on biologically-plausible microstructural tissue property changes (Weiskopf et al. 2013). Behaviorally relevant brain changes in iron-sensitive R2* were found in the occipital cortex and in the hippocampus (non-significant trend). In addition, in the occipital cortex, R2* increased during the

training period, and this increase was positively correlated with interindividual differences in balance learning rate, while the opposite pattern (R2* decrease and negative correlation with learning rate) was found in the hippocampus. These training-induced changes in R2* bear a resemblance to aging-related

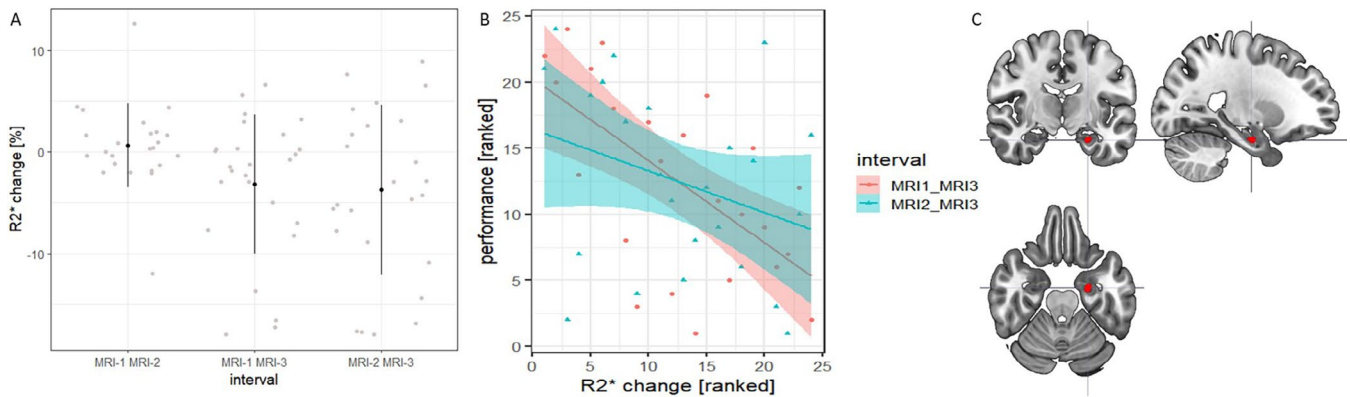


FIGURE 3 | Trend-level NPC results for R2 in the left HC*: (A) Scatter plots with mean values (± 1 SD) of the R2* value changes in the sample ($n = 26$) across the three measurement points, B: Correlation between DBT performance (learning rate) and within-cluster change of R2*, C: Location of the cluster in the left HC, peak voxel xyz ($-24, -11, -24$; $p = 0.055$, FWE-corrected, MNI152 space).

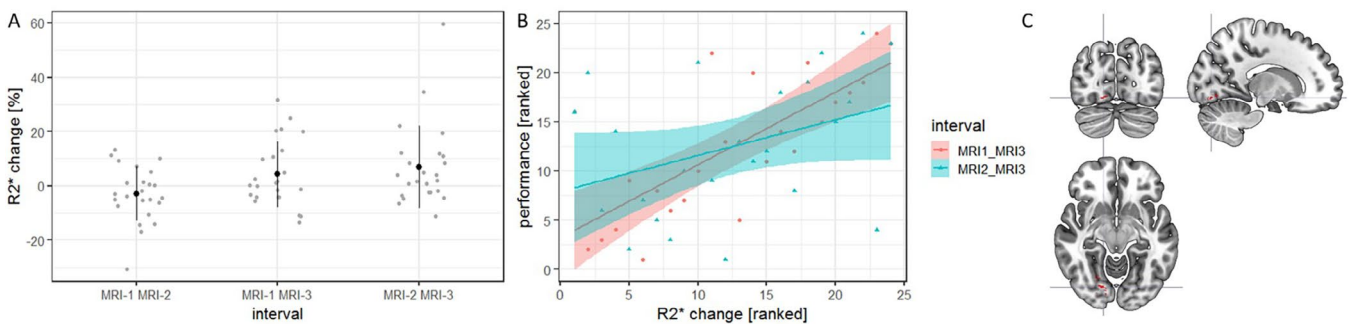


FIGURE 4 | Significant NPC results for R2* in the fusiform gyrus. (A) Scatter plots of within-cluster raw value changes for each participant ($n = 24$) are shown as gray dots, mean values (± 1 SD) overlaid. (B) Correlation of DBT performance (learning rate) and R2*s changes. Note that these Pearson correlation coefficients are not used for statistical inference, but only to show the direction of the relationships. (C) Shows the location of the significant cluster in the right fusiform gyrus rendered to MNI (MNI152 template), peak voxel xyz ($15, -78, -10$).

patterns of iron deficiency and deposition observed in both cortical and subcortical regions (Del C Valdés Hernández et al. 2015; Taubert et al. 2020). Iron accumulation is a common feature of the aging brain and is often regarded as a potential indicator of neurodegenerative conditions like Parkinson's disease (Cabrera-Valdivia et al. 1994; Kaindlstorfer et al. 2018; Krajcovicova, Klobusiakova, and Rektorova 2019; Sofic et al. 1988). However, the sensitivity of R2* to iron seems different depending on brain regions and tissue types (Kirilina et al. 2020) suggesting that different directions of training-induced R2* change in young adults may not reflect one and the same underlying mechanism operating in different directions. Thus, further long-term training studies in older adults are required in order to dissociate between R2* changes mimicking dynamic, short-term plasticity processes equivalent to those seen in young adults and/or a reversal of stable, long-term age-related changes in brain iron content. Furthermore, using ROI analyses, we found limited evidence for training-related microstructural changes in prefrontal and motor-related brain areas. A training-induced decrease in myelin-sensitive MT_{sat} in the medial prefrontal cortex is discussed in relation to myelin.

Accumulation of iron, particularly in subcortical gray matter regions, is associated with various neurodegenerative diseases and

age-related cognitive decline (Spence, McNeil, and Waiter 2020). However, iron is also essential for (re)myelination and repair processes (Carlson et al. 2007; Schulz, Kroner, and David 2012; Stephenson et al. 2014; Todorich et al. 2009; Tran et al. 2015). During aging, higher R2* values may indicate age-related iron deposition in subcortical brain regions while lower R2* values in the cortex could reflect iron reductions associated with atrophy and demyelination (Taubert et al. 2020). It was recently found that reduced R2* in the hippocampus is associated with higher physical activity levels (Lee et al. 2023) and the hippocampus is involved in early stages of learning (Gheysen et al. 2010). A training-related decrease in hippocampal iron content might be associated with synaptogenesis (Azzarito et al. 2023; Carlson et al. 2007; Tran et al. 2015) in the context of balance training (Dordevic et al. 2018; Sehm et al. 2014). These results are exploratory in nature and therefore require further confirmation. In particular, it could be tested whether training is able to alleviate iron-related deficits associated with physiological aging or neurodegeneration. However, it is important to note that the specific patterns of iron-related changes in R2* may differ between young and older adults. Our study exclusively involved young, healthy volunteers, and the observed R2* changes in this group may reflect dynamic, short-term plasticity processes rather than the more stable, long-term changes seen in aging. Therefore,

while our findings provide a conceptual link to aging-related iron deposition patterns, we acknowledge that direct comparisons should be made cautiously, given the differing baseline conditions and mechanisms between young and older brains. Further research is needed to determine whether the plasticity processes observed in young adults are consistent with those in aging populations, and this is currently being investigated in ongoing studies.

During skilled whole-body movements (e.g., locomotion, postural control), the associated sensations are predicted based on an internal forward model of the causes of sensory input (Keller and Mrcic-Flogel 2018). Such sensorimotor interactions are established and updated during the learning of new (whole-body) motor tasks. On the one hand, the newly acquired motor commands trigger sensory representations in the respective sensory brain areas and, on the other hand, dynamic whole-body postural control strongly depends on efficient multisensory predictive processing to link the different inputs from relevant sensory modalities (e.g., visual, vestibular, proprioceptive, tactile). In this respect, visual input processing is essential for postural control in general and for the stabilometer balance task in particular. One reason for this is that the participant stands on a seesaw-like, moving stabilometer platform, which generates significantly lower ground reaction forces, and thereby less tactile and proprioceptive sensations in the event of perturbations than a static platform. Thus, postural control probably relies more on visual and vestibular modalities. Our qualitative observations support this because participants closing their eyes during a stabilometer trial show an immediate drop in performance (referred to the study by Rogge et al. (2017)) (Muelas Pérez et al. 2014). Motor learning of the stabilometer balance task leads, among other things, to neural changes in visuomotor areas of the parietal cortex and in visual areas of the occipital cortex (Taubert et al. 2010). In the present study, an $R2^*$ signal increase was observable in the left fusiform gyrus, and between-participant variation in $R2^*$ change was correlated with the learning rate of the DBT. This finding was obtained in an exploratory whole-brain analysis, which is why the role of this particular visual area in the balance learning process must be further substantiated/confirmed in future studies. However, it is noteworthy that the left fusiform area has already been linked to complex movement coordination in other studies (Karabanov et al. 2023).

Training-induced changes in myelin have been explored in a few studies using measures of relaxation time and/or magnetization transfer (Lakhani et al. 2016; Matuszewski et al. 2021; Wenger, Brozzoli et al. 2017; Wenger, Kühn et al. 2017). Matuszewski et al. (2021) observed increases in R1 after 8 months of somatosensory tactile reading training within the left and right ventral occipitotemporal cortex. Following 4 weeks of practice in a virtual reality training paradigm, Lakhani et al. (2016) noted increases in myelin water fraction (MWF) within the left intraparietal sulcus and left parieto-occipital sulcus. Interestingly, the intraparietal sulcus exhibited a negative correlation with the rate of motor skill acquisition. Their conclusion suggested that a slower learning rate results in greater neuroplastic changes (Lakhani et al. 2016), which is not in line with our finding of a positive correlation between learning and $R2^*$ increases. The neuroplastic response to training is highly task-specific, and

differences in task design, the timing of task-related demands on the brain, and varying training volumes between MRI scans have led to different results. In other studies utilizing MPM, initial decreases in $R2^*$, MT_{sat} , and R1 were observed after 7 days, followed by an increase after 28 days of training using a motor skill learning paradigm (Azzarito et al. 2023). Changes were noted in the left cerebellum, right hippocampus, and left internal capsule. MPMs were also employed to explore changes during cognitive training (Biel et al. 2020; Ziminski et al. 2023). While three of these studies demonstrated training-induced microstructural tissue changes in correlation with behavioral performance (Azzarito et al. 2023; Lakhani et al. 2016; Matuszewski et al. 2021), others have failed to show significant training-induced qMRI alterations with behavioral change (Biel et al. 2020). The former potentially reflects a sensitivity of quantitative structural metrics to the high inter-individual variability of training responses. At the same time, it also highlights the challenges in interpreting potential underlying mechanisms of qMRI changes in different training domains. Therefore, it seems important to improve the comparability of study results, for example, through the joint analysis of multimodal data. This will support conclusions about latent biological processes of plasticity on the basis of the differential information from various structural metrics.

Myelin in the brain primarily serves to enhance the conduction velocity along axons, facilitating rapid transmission over long distances within the brain (Freeman et al. 2016; Freeman et al. 2015). Regional differences in intra-cortical myelin content have been demonstrated in the human gray matter, potentially fine-tuning local neuronal circuits (Glasser et al. 2014) and modulating neuroplasticity on a rapid temporal scale (Azzarito et al. 2023). MT_{sat} and R1 are acknowledged as surrogate markers of myelin content in the cortex (Georgiadis et al. 2021; Heath et al. 2018; Natu et al. 2019; Schmierer et al. 2004). Given that training induces changes in synaptogenesis within the gray matter, an initial decrease in myelin-sensitive R1 and MT_{sat} due to the inhibitory effect of myelin on cortical synaptic plasticity could be expected and considered plausible (Bacmeister et al. 2022; McGee et al. 2005). Though speculative, the MT_{sat} decrease in MFC could result from a relative reduction in myelin and the formation of new synapses or unmyelinated connections. Subsequently, redundant connections are eliminated during the pruning phase (Kantor and Kolodkin 2003; Yasuda et al. 2011) and activity-dependent myelination of established connections can occur (Fields 2015; Sampaio-Baptista and Johansen-Berg 2017). The non-significant increase in R1 in the very same region (Figure 2) suggests a potential reduction solely in the overall proportion of myelin content due to a lower proportion of myelin-related tissue among the observed tissue increase. This is supported by the observed decrease in proton density (PD), which negatively correlates with the increase in R1, possibly indicating tissue augmentation concurrent with reduced water content. The simultaneous shifts in PD and R1 appear to be driven by this water-related process. Notably, PD and R1 share ~33% variance, providing an additional rationale for their correlation (Carter et al. 2022).

We encountered several limitations in this study. First, the absence of an independent control group prompted us to utilize

the initial period without intervention as a quasi-control condition. We attribute our results to training-related effects in the left MFG and left MFC because a direct interaction with the learning task was necessary to induce neuroplasticity, whereas comparable changes did not occur in the control phase of the experiment. MPMs are suited for use in longitudinal studies because they are highly reliable (Aye et al. 2022). Second, in considering the absence of significant structural changes in the supplementary motor area (SMA) in this study, it is important to acknowledge that our study design did not include MRI measurements during the early learning phase of the balance training (DBT) task. This is a potential limitation, as previous studies, such as those by Taubert et al. (2010) and Wenger, Kühn et al. (2017), have highlighted that morphometric gray matter changes are likely larger in the early phase of motor skill learning. Wenger, Kühn et al. (2017) propose that gray matter expansion occurs predominantly during the initial phase of motor learning, followed by a process of renormalization as the skill becomes more automated and efficient. These dynamics suggest that the most pronounced volumetric changes in gray matter might occur shortly after the onset of training, potentially explaining why our study, which did not capture this early phase, did not observe significant changes in regions like the SMA. Taubert et al. (2010) similarly reported early training-induced changes in the SMA, reinforcing the idea that this region is particularly responsive during the initial stages of motor skill learning. Our study focused on measuring microstructural changes after the completion of the intervention, which might have missed these early, transient changes. Furthermore, diffusion-related (microstructural) white matter changes tended to increase with training time in Taubert et al. (2010) and diffusion-related cortical brain changes in SMA were also present in this particular sample (Lehmann et al. 2023). Microstructural changes as measured with the MPM protocol and related to motor learning were present in visual areas and the hippocampus (Figures 3 and 4). Thus, the results of our studies suggest a differential sensitivity of MPM and (advanced) diffusion metrics to training-induced brain changes in the later practice period (e.g., beyond the initial period of skill acquisition) as well as a higher likelihood to detect morphometric gray matter changes in the early period of skill acquisition. This highlights the importance of including additional measurement points, particularly during the early stages of training, to capture the temporal dynamics of neuroplastic changes. The increased training volume in the present study compared to Taubert et al. (2010) might have accelerated the learning process, potentially leading to a quicker onset of morphometric gray matter expansion followed by earlier renormalization. Thirdly, while $R1$, $R2^*$, and MT_{sat} are increasingly regarded as proxies for central nervous system microstructure and (strongly) correlate with histological myelin markers (Natu et al. 2019; Tofts 2003; Weber et al. 2020), they still represent indirect estimations of microstructure. Fourthly, optimal task selection for a neuroplasticity study is a challenge because experimental control usually trades-off with task complexity and a sufficient level of task difficulty to trigger plasticity. As well as reducing the intervention duration from 6 (Taubert et al. 2010) to 4 weeks (while increasing the number of training sessions) might have influenced our study results.

6 | Conclusion

Our study provides new insights into changes in quantitative cortical tissue properties that are relevant in the context of aging and neurodegeneration. While training-induced changes in myelin-related qMRI metrics (MT_{sat}) were limited to medial prefrontal regions, occipital changes in an iron-related marker ($R2^*$) were additionally correlated with behavioral improvements during training. As the latter result was identified in exploratory whole-brain analysis, this may encourage future attempts to confirm cortical $R2^*$ changes in hypothesis-driven approaches because modifiable biomarkers for iron deficiency seem highly relevant in the clinical context. For longitudinal research into training-induced plasticity of the human brain, a combination of cortical diffusion and qMRI approaches seems promising to test for behaviorally-specific and biologically-relevant brain changes in response to training.

Acknowledgments

Open Access funding enabled and organized by Projekt DEAL.

Author Contributions

Norman Aye: conceptualization, methodology, investigation, project administration, writing – original draft, visualization, data curation, formal analysis. **Nico Lehmann:** conceptualization, methodology, investigation, writing – review and editing. **Jörn Kaufmann:** methodology, investigation, data curation, writing – review and editing. **Hans-Jochen Heinze:** resources. **Emrah Düzel:** conceptualization, resources. **Gabriel Ziegler:** conceptualization, methodology, writing – review and editing. **Marco Taubert:** conceptualization, methodology, writing – review and editing, supervision, project administration, funding acquisition.

Conflicts of Interest

The authors declare no conflicts of interest.

Data Availability Statement

The data that support the findings of this study are available from the corresponding author upon reasonable request.

References

- Adams, J. A. 1987. “Historical Review and Appraisal of Research on the Learning, Retention, and Transfer of Human Motor Skills.” *Psychological Bulletin* 101: 41–74. <https://doi.org/10.1037/0033-2909.101.1.41>.
- Asan, L., C. Falfán-Melgoza, C. A. Beretta, et al. 2021. “Cellular Correlates of Gray Matter Volume Changes in Magnetic Resonance Morphometry Identified by Two-Photon Microscopy.” *Scientific Reports* 11: 4234. <https://doi.org/10.1038/s41598-021-83491-8>.
- Ashburner, J. 2007. “A Fast Diffeomorphic Image Registration Algorithm.” *NeuroImage* 38: 95–113. <https://doi.org/10.1016/j.neuroimage.2007.07.007>.
- Ashburner, J., and K. J. Friston. 2005. “Unified Segmentation.” *NeuroImage* 26: 839–851. <https://doi.org/10.1016/j.neuroimage.2005.02.018>.
- Aye, N., N. Lehmann, J. Kaufmann, et al. 2022. “Test-Retest Reliability of Multi-Parametric Maps (MPM) of Brain Microstructure.” *NeuroImage* 256: 119249. <https://doi.org/10.1016/j.neuroimage.2022.119249>.

- Azzarito, M., T. M. Emmenegger, G. Ziegler, et al. 2023. "Coherent, Time-Shifted Patterns of Microstructural Plasticity During Motor-Skill Learning." *NeuroImage* 274: 120128. <https://doi.org/10.1016/j.neuroimage.2023.120128>.
- Bacmeister, C. M., R. Huang, L. A. Osso, et al. 2022. "Motor Learning Drives Dynamic Patterns of Intermittent Myelination on Learning-Activated Axons." *Nature Neuroscience* 25: 1300–1313. <https://doi.org/10.1038/s41593-022-01169-4>.
- Barbosa, J. H. O., A. C. Santos, V. Tumas, et al. 2015. "Quantifying Brain Iron Deposition in Patients With Parkinson's Disease Using Quantitative Susceptibility Mapping, R2 and R2*." *Magnetic Resonance Imaging* 33: 559–565. <https://doi.org/10.1016/j.mri.2015.02.021>.
- Biel, D., T. K. Steiger, T. Volkmann, N. Jochems, and N. Bunzeck. 2020. "The Gains of a 4-Week Cognitive Training Are Not Modulated by Novelty." *Human Brain Mapping* 41: 2596–2610. <https://doi.org/10.1002/hbm.24965>.
- Boyke, J., J. Driemeyer, C. Gaser, C. Büchel, and A. May. 2008. "Training-Induced Brain Structure Changes in the Elderly." *Journal of Neuroscience* 28: 7031–7035. <https://doi.org/10.1523/JNEUROSCI.0742-08.2008>.
- Cabrera-Valdivia, F., F. J. Jiménez-Jiménez, J. A. Molina, et al. 1994. "Peripheral Iron Metabolism in Patients With Parkinson's Disease." *Journal of the Neurological Sciences* 125: 82–86.
- Callaghan, M. F., O. Josephs, M. Herbst, M. Zaitsev, N. Todd, and N. Weiskopf. 2015. "An Evaluation of Prospective Motion Correction (PMC) for High Resolution Quantitative MRI." *Frontiers in Neuroscience* 9: 97. <https://doi.org/10.3389/fnins.2015.00097>.
- Campbell, J. S. W., I. R. Leppert, S. Narayanan, et al. 2018. "Promise and Pitfalls of g-Ratio Estimation With MRI." *NeuroImage* 182: 80–96. <https://doi.org/10.1016/j.neuroimage.2017.08.038>.
- Carey, D., F. Caprini, M. Allen, et al. 2018. "Quantitative MRI Provides Markers of Intra-, Inter-Regional, and Age-Related Differences in Young Adult Cortical Microstructure." *NeuroImage* 182: 429–440. <https://doi.org/10.1016/j.neuroimage.2017.11.066>.
- Carlson, E. S., J. D. H. Stead, C. R. Neal, A. Petryk, and M. K. Georgieff. 2007. "Perinatal Iron Deficiency Results in Altered Developmental Expression of Genes Mediating Energy Metabolism and Neuronal Morphogenesis in Hippocampus." *Hippocampus* 17: 679–691. <https://doi.org/10.1002/hipo.20307>.
- Carter, F., A. Anwender, T. Goucha, et al. 2022. *Assessing Quantitative MRI Techniques Using Multimodal Comparisons*, 32. Cold Spring Harbor Laboratory. bioRxiv. <https://doi.org/10.1101/2022.02.10.479780>.
- Cercignani, M., and G. J. Barker. 2008. "A Comparison Between Equations Describing In Vivo MT: The Effects of Noise and Sequence Parameters." *Journal of Magnetic Resonance* 191: 171–183. <https://doi.org/10.1016/j.jmr.2007.12.012>.
- Del C Valdés Hernández, M., S. Ritchie, A. Glatz, et al. 2015. "Brain Iron Deposits and Lifespan Cognitive Ability." *Age (Dordrecht, Netherlands)* 37: 100. <https://doi.org/10.1007/s11357-015-9837-2>.
- Della-Maggiore, V., J. Scholz, H. Johansen-Berg, and T. Paus. 2009. "The Rate of Visuomotor Adaptation Correlates With Cerebellar White-Matter Microstructure." *Human Brain Mapping* 30: 4048–4053. <https://doi.org/10.1002/hbm.20828>.
- Dordevic, M., R. Schrader, M. Taubert, P. Müller, A. Hökelmann, and N. G. Müller. 2018. "Vestibulo-Hippocampal Function Is Enhanced and Brain Structure Altered in Professional Ballet Dancers." *Frontiers in Integrative Neuroscience* 12: 50. <https://doi.org/10.3389/fnint.2018.00050>.
- Draganski, B., J. Ashburner, C. Hutton, et al. 2011. "Regional Specificity of MRI Contrast Parameter Changes in Normal Ageing Revealed by Voxel-Based Quantification (VBQ)." *NeuroImage* 55: 1423–1434. <https://doi.org/10.1016/j.neuroimage.2011.01.052>.
- Draganski, B., C. Gaser, V. Busch, G. Schuierer, U. Bogdahn, and A. May. 2004. "Neuroplasticity: Changes in Grey Matter Induced by Training." *Nature* 427: 311–312. <https://doi.org/10.1038/427311a>.
- Draganski, B., C. Gaser, G. Kempermann, et al. 2006. "Temporal and Spatial Dynamics of Brain Structure Changes During Extensive Learning." *Journal of Neuroscience* 26: 6314–6317. <https://doi.org/10.1523/JNEUROSCI.4628-05.2006>.
- Draganski, B., and F. Kherif. 2013. "In Vivo Assessment of Use-Dependent Brain Plasticity—Beyond the "One Trick Pony" Imaging Strategy." *NeuroImage* 73: 255–259; discussion 265–7. <https://doi.org/10.1016/j.neuroimage.2012.08.058>.
- Edwards, L. J., E. Kirilina, S. Mohammadi, and N. Weiskopf. 2018. "Microstructural Imaging of Human Neocortex In Vivo." *NeuroImage* 182: 184–206. <https://doi.org/10.1016/j.neuroimage.2018.02.055>.
- Fatouros, P. P., and A. Marmarou. 1999. "Use of Magnetic Resonance Imaging for In Vivo Measurements of Water Content in Human Brain: Method and Normal Values." *Journal of Neurosurgery* 90: 109–115. <https://doi.org/10.3171/jns.1999.90.1.0109>.
- Fatouros, P. P., A. Marmarou, K. A. Kraft, S. Inao, and F. P. Schwarz. 1991. "In Vivo Brain Water Determination by T1 Measurements: Effect of Total Water Content, Hydration Fraction, and Field Strength." *Magnetic Resonance in Medicine* 17: 402–413. <https://doi.org/10.1002/mrm.1910170212>.
- Fields, R. D. 2015. "A New Mechanism of Nervous System Plasticity: Activity-Dependent Myelination." *Nature Reviews. Neuroscience* 16: 756–767. <https://doi.org/10.1038/nrn4023>.
- Finch, H. 2005. "Comparison of the Performance of Nonparametric and Parametric MANOVA Test Statistics When Assumptions Are Violated." *Methodology* 1: 27–38. <https://doi.org/10.1027/1614-1881.1.1.27>.
- Fisher, R. A. 1933. "Statistical Methods for Research Workers." *Nature* 131: 383. <https://doi.org/10.1038/131383b0>.
- Fox, P. W., S. L. Hershberger, and T. J. Bouchard. 1996. "Genetic and Environmental Contributions to the Acquisition of a Motor Skill." *Nature* 384: 356–358. <https://doi.org/10.1038/384356a0>.
- Freeman, S. A., A. Desmazières, D. Fricker, C. Lubetzki, and N. Sol-Foulon. 2016. "Mechanisms of Sodium Channel Clustering and Its Influence on Axonal Impulse Conduction." *Cellular and Molecular Life Sciences* 73: 723–735. <https://doi.org/10.1007/s00018-015-2081-1>.
- Freeman, S. A., A. Desmazières, J. Simonnet, et al. 2015. "Acceleration of Conduction Velocity Linked to Clustering of Nodal Components Precedes Myelination." *Proceedings of the National Academy of Sciences of the United States of America* 112: E321–E328. <https://doi.org/10.1073/pnas.1419099112>.
- Gelman, N., J. R. Ewing, J. M. Gorell, E. M. Spickler, and E. G. Solomon. 2001. "Interregional Variation of Longitudinal Relaxation Rates in Human Brain at 3.0 T: Relation to Estimated Iron and Water Contents." *Magnetic Resonance in Medicine* 45: 71–79. [https://doi.org/10.1002/1522-2594\(200101\)45:1<71::aid-mrm1011>3.0.co;2-2](https://doi.org/10.1002/1522-2594(200101)45:1<71::aid-mrm1011>3.0.co;2-2).
- Georgiadis, M., A. Schroeter, Z. Gao, et al. 2021. "Nanostucture-Specific X-Ray Tomography Reveals Myelin Levels, Integrity and Axon Orientations in Mouse and Human Nervous Tissue." *Nature Communications* 12: 2941. <https://doi.org/10.1038/s41467-021-22719-7>.
- Ghadery, C., L. Pirpamer, E. Hofer, et al. 2015. "R2* Mapping for Brain Iron: Associations With Cognition in Normal Aging." *Neurobiology of Aging* 36: 925–932. <https://doi.org/10.1016/j.neurobiolaging.2014.09.013>.
- Gheysen, F., F. van Opstal, C. Roggeman, H. van Waelvelde, and W. Fias. 2010. "Hippocampal Contribution to Early and Later Stages of Implicit Motor Sequence Learning." *Experimental Brain Research* 202: 795–807. <https://doi.org/10.1007/s00221-010-2186-6>.
- Glasser, M. F., M. S. Goyal, T. M. Preuss, M. E. Raichle, and D. C. van Essen. 2014. "Trends and Properties of Human Cerebral Cortex:

- Correlations With Cortical Myelin Content." *NeuroImage* 93, no. Pt 2: 165–175. <https://doi.org/10.1016/j.neuroimage.2013.03.060>.
- Green, C. S., and D. Bavelier. 2008. "Exercising Your Brain: A Review of Human Brain Plasticity and Training-Induced Learning." *Psychology and Aging* 23: 692–701. <https://doi.org/10.1037/a0014345>.
- Heath, F., S. A. Hurley, H. Johansen-Berg, and C. Sampaio-Baptista. 2018. "Advances in Noninvasive Myelin Imaging." *Developmental Neurobiology* 78: 136–151. <https://doi.org/10.1002/dneu.22552>.
- Helms, G., H. Dathe, and P. Dechent. 2010. "Modeling the Influence of TR and Excitation Flip Angle on the Magnetization Transfer Ratio (MTR) in Human Brain Obtained From 3D Spoiled Gradient Echo MRI." *Magnetic Resonance in Medicine* 64: 177–185. <https://doi.org/10.1002/mrm.22379>.
- Helms, G., H. Dathe, N. Weiskopf, and P. Dechent. 2011. "Identification of Signal Bias in the Variable Flip Angle Method by Linear Display of the Algebraic Ernst Equation." *Magnetic Resonance in Medicine* 66: 669–677. <https://doi.org/10.1002/mrm.22849>.
- Helms, G., B. Draganski, R. Frackowiak, J. Ashburner, and N. Weiskopf. 2009. "Improved Segmentation of Deep Brain Grey Matter Structures Using Magnetization Transfer (MT) Parameter Maps." *NeuroImage* 47: 194–198. <https://doi.org/10.1016/j.neuroimage.2009.03.053>.
- Henkelman, R. M., X. Huang, Q. S. Xiang, G. J. Stanisz, S. D. Swanson, and M. J. Bronskill. 1993. "Quantitative Interpretation of Magnetization Transfer." *Magnetic Resonance in Medicine* 29: 759–766. <https://doi.org/10.1002/mrm.1910290607>.
- Henkelman, R. M., G. J. Stanisz, and S. J. Graham. 2001. "Magnetization Transfer in MRI: A Review." *NMR in Biomedicine* 14: 57–64. <https://doi.org/10.1002/nbm.683>.
- Kaindlstorfer, C., K. A. Jellinger, S. Eschlböck, N. Stefanova, G. Weiss, and G. K. Wenning. 2018. "The Relevance of Iron in the Pathogenesis of Multiple System Atrophy: A Viewpoint." *Journal of Alzheimer's Disease* 61: 1253–1273. <https://doi.org/10.3233/JAD-170601>.
- Kantor, D. B., and A. L. Kolodkin. 2003. "Curbing the Excesses of Youth: Molecular Insights Into Axonal Pruning." *Neuron* 38: 849–852. [https://doi.org/10.1016/s0896-6273\(03\)00364-7](https://doi.org/10.1016/s0896-6273(03)00364-7).
- Karabanov, A. N., G. Chillemi, K. H. Madsen, and H. R. Siebner. 2023. "Dynamic Involvement of Premotor and Supplementary Motor Areas in Bimanual Pinch Force Control." *NeuroImage* 276: 120203. <https://doi.org/10.1016/j.neuroimage.2023.120203>.
- Keller, G. B., and T. D. Mrsic-Flogel. 2018. "Predictive Processing: A Canonical Cortical Computation." *Neuron* 100: 424–435. <https://doi.org/10.1016/j.neuron.2018.10.003>.
- Kheirbek, M. A., L. J. Drew, N. S. Burghardt, et al. 2013. "Differential Control of Learning and Anxiety Along the Dorsoventral Axis of the Dentate Gyrus." *Neuron* 77: 955–968. <https://doi.org/10.1016/j.neuron.2012.12.038>.
- Kirilina, E., S. Helbling, M. Morawski, et al. 2020. "Superficial White Matter Imaging: Contrast Mechanisms and Whole-Brain In Vivo Mapping." *Science Advances* 6: 9281. <https://doi.org/10.1126/sciadv.aaz9281>.
- Knief, U., and W. Forstmeier. 2021. "Violating the Normality Assumption May Be the Lesser of Two Evils." *Behavior Research Methods* 53: 2576–2590. <https://doi.org/10.3758/s13428-021-01587-5>.
- Konorski, J. 1949. "Conditioned Reflexes and Neuron Organization." *Journal of the American Medical Association* 139: 1045. <https://doi.org/10.1001/jama.1949.02900320075040>.
- Krajcovicova, L., P. Klobusiakova, and I. Rektorova. 2019. "Gray Matter Changes in Parkinson's and Alzheimer's Disease and Relation to Cognition." *Current Neurology and Neuroscience Reports* 19: 85. <https://doi.org/10.1007/s11910-019-1006-z>.
- Lakhani, B., M. R. Borich, J. N. Jackson, et al. 2016. "Motor Skill Acquisition Promotes Human Brain Myelin Plasticity." *Neural Plasticity* 2016: 7526135. <https://doi.org/10.1155/2016/7526135>.
- Langkammer, C., N. Krebs, W. Goessler, et al. 2010. "Quantitative MR Imaging of Brain Iron: A Postmortem Validation Study." *Radiology* 257: 455–462. <https://doi.org/10.1148/radiol.10100495>.
- Langkammer, C., T. Liu, M. Khalil, et al. 2013. "Quantitative Susceptibility Mapping in Multiple Sclerosis." *Radiology* 267: 551–559. <https://doi.org/10.1148/radiol.12120707>.
- Lee, S. Y., E. W. Paolillo, R. Saloner, et al. 2023. "Moderating Role of Physical Activity on Hippocampal Iron Deposition and Memory Outcomes in Typically Aging Older Adults." *Neurobiology of Aging* 131: 124–131. <https://doi.org/10.1016/j.neurobiolaging.2023.07.026>.
- Lehmann, N., N. Aye, J. Kaufmann, et al. 2021. "Longitudinal Reproducibility of Neurite Orientation Dispersion and Density Imaging (NODDI) Derived Metrics in the White Matter." *Neuroscience* 457: 165–185. <https://doi.org/10.1016/j.neuroscience.2021.01.005>.
- Lehmann, N., N. Aye, J. Kaufmann, et al. 2023. "Changes in Cortical Microstructure of the Human Brain Resulting From Long-Term Motor Learning." *Journal of Neuroscience* 43: 8637–8648. <https://doi.org/10.1523/JNEUROSCI.0537-23.2023>.
- Lehmann, N., A. Villringer, and M. Taubert. 2020. "Colocalized White Matter Plasticity and Increased Cerebral Blood Flow Mediate the Beneficial Effect of Cardiovascular Exercise on Long-Term Motor Learning." *Journal of Neuroscience* 40: 2416–2429. <https://doi.org/10.1523/JNEUROSCI.2310-19.2020>.
- Lehmann, N., A. Villringer, and M. Taubert. 2022. "Priming Cardiovascular Exercise Improves Complex Motor Skill Learning by Affecting the Trajectory of Learning-Related Brain Plasticity." *Scientific Reports* 12: 1107. <https://doi.org/10.1038/s41598-022-05145-7>.
- Lema, A., C. Bishop, O. Malik, et al. 2017. "A Comparison of Magnetization Transfer Methods to Assess Brain and Cervical Cord Microstructure in Multiple Sclerosis." *Journal of Neuroimaging* 27: 221–226. <https://doi.org/10.1111/jon.12377>.
- Leutritz, T., M. Seif, G. Helms, et al. 2020. "Multiparameter Mapping of Relaxation (R1, R2*), Proton Density and Magnetization Transfer Saturation at 3 T: A Multicenter Dual-Vendor Reproducibility and Repeatability Study." *Human Brain Mapping* 41: 4232–4247. <https://doi.org/10.1002/hbm.25122>.
- Lorio, S., A. Lutti, F. Kherif, et al. 2014. "Disentangling In Vivo the Effects of Iron Content and Atrophy on the Ageing Human Brain." *NeuroImage* 103: 280–289. <https://doi.org/10.1016/j.neuroimage.2014.09.044>.
- Lövdén, M., L. Bäckman, U. Lindenberger, S. Schaefer, and F. Schmiedek. 2010. "A Theoretical Framework for the Study of Adult Cognitive Plasticity." *Psychological Bulletin* 136: 659–676. <https://doi.org/10.1037/a0020080>.
- Lövdén, M., E. Wenger, J. Mårtensson, U. Lindenberger, and L. Bäckman. 2013. "Structural Brain Plasticity in Adult Learning and Development." *Neuroscience and Biobehavioral Reviews* 37: 2296–2310. <https://doi.org/10.1016/j.neubiorev.2013.02.014>.
- Lutti, A., F. Dick, M. I. Sereno, and N. Weiskopf. 2014. "Using High-Resolution Quantitative Mapping of R1 as an Index of Cortical Myelination." *NeuroImage* 93, no. Pt 2: 176–188. <https://doi.org/10.1016/j.neuroimage.2013.06.005>.
- Lutti, A., C. Hutton, J. Finsterbusch, G. Helms, and N. Weiskopf. 2010. "Optimization and Validation of Methods for Mapping of the Radiofrequency Transmit Field at 3T." *Magnetic Resonance in Medicine* 64: 229–238. <https://doi.org/10.1002/mrm.22421>.
- Lutti, A., J. Stadler, O. Josephs, et al. 2012. "Robust and Fast Whole Brain Mapping of the RF Transmit Field B1 at 7T." *PLoS One* 7: e32379. <https://doi.org/10.1371/journal.pone.0032379>.

- Matuszewski, J., B. Kossowski, Ł. Bola, et al. 2021. "Brain Plasticity Dynamics During Tactile Braille Learning in Sighted Subjects: Multi-Contrast MRI Approach." *NeuroImage* 227: 117613. <https://doi.org/10.1016/j.neuroimage.2020.117613>.
- Mazziotta, J., A. Toga, A. Evans, et al. 2001a. "A Probabilistic Atlas and Reference System for the Human Brain: International Consortium for Brain Mapping (ICBM). Philosophical Transactions of the Royal Society of London." *Series B, Biological Sciences* 356: 1293–1322. <https://doi.org/10.1098/rstb.2001.0915>.
- Mazziotta, J., A. Toga, A. Evans, et al. 2001b. "A Four-Dimensional Probabilistic Atlas of the Human Brain." *Journal of the American Medical Informatics Association* 8: 401–430. <https://doi.org/10.1136/jamia.2001.0080401>.
- Mazziotta, J. C., A. W. Toga, A. Evans, P. Fox, and J. Lancaster. 1995. "A Probabilistic Atlas of the Human Brain: Theory and Rationale for Its Development. The International Consortium for Brain Mapping (ICBM)." *NeuroImage* 2: 89–101. <https://doi.org/10.1006/nimg.1995.1012>.
- McGee, A. W., Y. Yang, Q. S. Fischer, N. W. Daw, and S. M. Strittmatter. 2005. "Experience-Driven Plasticity of Visual Cortex Limited by Myelin and Nogo Receptor." *Science (New York, N.Y.)* 309: 2222–2226. <https://doi.org/10.1126/science.1114362>.
- McNevin, N. H., C. H. Shea, and G. Wulf. 2003. "Increasing the Distance of an External Focus of Attention Enhances Learning." *Psychological Research* 67: 22–29. <https://doi.org/10.1007/s00426-002-0093-6>.
- Muelas Pérez, R., R. Sabido Solana, D. Barbado Murillo, and F. J. Moreno Hernández. 2014. "Visual Availability, Balance Performance and Movement Complexity in Dancers." *Gait & Posture* 40: 556–560. <https://doi.org/10.1016/j.gaitpost.2014.06.021>.
- Natu, V. S., J. Gomez, M. Barnett, et al. 2019. "Apparent Thinning of Human Visual Cortex During Childhood Is Associated With Myelination." *Proceedings of the National Academy of Sciences of the United States of America* 116: 20750–20759. <https://doi.org/10.1073/pnas.1904931116>.
- Nazeri, A., M. M. Chakravarty, D. J. Rotenberg, et al. 2015. "Functional Consequences of Neurite Orientation Dispersion and Density in Humans Across the Adult Lifespan." *Journal of Neuroscience* 35: 1753–1762. <https://doi.org/10.1523/JNEUROSCI.3979-14.2015>.
- Nierhaus, T., C. Vidaurre, C. Sannelli, K.-R. Mueller, and A. Villringer. 2021. "Immediate Brain Plasticity After One Hour of Brain-Computer Interface (BCI)." *Journal of Physiology* 599: 2435–2451. <https://doi.org/10.1113/JP278118>.
- Olivo, G., M. Lövdén, A. Manzouri, et al. 2022. "Estimated Gray Matter Volume Rapidly Changes After a Short Motor Task." *Cerebral Cortex* 32: 4356–4369. <https://doi.org/10.1093/cercor/bhab488>.
- Orrell, A. J., F. F. Eves, and R. S. W. Masters. 2006. "Implicit Motor Learning of a Balancing Task." *Gait & Posture* 23: 9–16. <https://doi.org/10.1016/j.gaitpost.2004.11.010>.
- Paillard, J. 1976. "Réflexions Sur L'usage Du Concept De Plasticité En Neurobiologie."
- Pizzagalli, F., G. Auzias, Q. Yang, et al. 2020. "The Reliability and Heritability of Cortical Folds and Their Genetic Correlations Across Hemispheres." *Communications Biology* 3: 510. <https://doi.org/10.1038/s42003-020-01163-1>.
- Rogge, A.-K., B. Röder, A. Zech, et al. 2017. "Balance Training Improves Memory and Spatial Cognition in Healthy Adults." *Scientific Reports* 7: 5661. <https://doi.org/10.1038/s41598-017-06071-9>.
- Rowley, C. D., N. A. Bock, R. Deichmann, et al. 2019. "Exercise and Microstructural Changes in the Motor Cortex of Older Adults." *European Journal of Neuroscience* 51: 1711–1722. <https://doi.org/10.1111/ejn.14585>.
- Sampaio-Baptista, C., and H. Johansen-Berg. 2017. "White Matter Plasticity in the Adult Brain." *Neuron* 96: 1239–1251. <https://doi.org/10.1016/j.neuron.2017.11.026>.
- Sampaio-Baptista, C., J. Scholz, M. Jenkinson, et al. 2014. "Gray Matter Volume Is Associated With Rate of Subsequent Skill Learning After a Long Term Training Intervention." *NeuroImage* 96: 158–166. <https://doi.org/10.1016/j.neuroimage.2014.03.056>.
- Schmierer, K., F. Scaravilli, D. R. Altmann, G. J. Barker, and D. H. Miller. 2004. "Magnetization Transfer Ratio and Myelin in Postmortem Multiple Sclerosis Brain." *Annals of Neurology* 56: 407–415. <https://doi.org/10.1002/ana.20202>.
- Schulz, K., A. Kroner, and S. David. 2012. "Iron Efflux From Astrocytes Plays a Role in Remyelination." *Journal of Neuroscience* 32: 4841–4847. <https://doi.org/10.1523/JNEUROSCI.5328-11.2012>.
- Sehm, B., M. Taubert, V. Conde, et al. 2014. "Structural Brain Plasticity in Parkinson's Disease Induced by Balance Training." *Neurobiology of Aging* 35: 232–239. <https://doi.org/10.1016/j.neurobiolaging.2013.06.021>.
- Shao, X., D. Luo, Y. Zhou, et al. 2022. "Myeloarchitectonic Plasticity in Elite Golf Players' Brains." *Human Brain Mapping* 43: 3461–3468. <https://doi.org/10.1002/hbm.25860>.
- Shea, C. H., and G. Wulf. 1999. "Enhancing Motor Learning Through External-Focus Instructions and Feedback." *Human Movement Science* 18: 553–571. [https://doi.org/10.1016/S0167-9457\(99\)00031-7](https://doi.org/10.1016/S0167-9457(99)00031-7).
- Smith, S. M., M. Jenkinson, H. Johansen-Berg, et al. 2006. "Tract-based Spatial Statistics: Voxelwise Analysis of Multi-Subject Diffusion Data." *NeuroImage* 31: 1487–1505. <https://doi.org/10.1016/j.neuroimage.2006.02.024>.
- Smith, S. M., and T. E. Nichols. 2009. "Threshold-Free Cluster Enhancement: Addressing Problems of Smoothing, Threshold Dependence and Localisation in Cluster Inference." *NeuroImage* 44: 83–98. <https://doi.org/10.1016/j.neuroimage.2008.03.061>.
- Sofic, E., P. Riederer, H. Heinsen, et al. 1988. "Increased Iron (III) and Total Iron Content in Post Mortem Substantia Nigra of Parkinsonian Brain." *Journal of Neural Transmission* 74: 199–205.
- Song, C., K. Sandberg, R. Rutiku, and R. Kanai. 2022. "Linking Human Behaviour to Brain Structure: Further Challenges and Possible Solutions." *Nature Reviews. Neuroscience* 23: 517–518. <https://doi.org/10.1038/s41583-022-00614-4>.
- Spence, H., C. J. McNeil, and G. D. Waiter. 2020. "The Impact of Brain Iron Accumulation on Cognition: A Systematic Review." *PLoS One* 15: e0240697. <https://doi.org/10.1371/journal.pone.0240697>.
- Stephenson, E., N. Nathoo, Y. Mahjoub, J. F. Dunn, and V. W. Yong. 2014. "Iron in Multiple Sclerosis: Roles in Neurodegeneration and Repair." *Nature Reviews. Neurology* 10: 459–468. <https://doi.org/10.1038/nrneuro.2014.118>.
- Surgent, O. J., O. I. Dadalko, K. A. Pickett, and B. G. Travers. 2019. "Balance and the Brain: A Review of Structural Brain Correlates of Postural Balance and Balance Training in Humans." *Gait & Posture* 71: 245–252. <https://doi.org/10.1016/j.gaitpost.2019.05.011>.
- Tabelow, K., E. Balteau, J. Ashburner, et al. 2019. "hMRI - A Toolbox for Quantitative MRI in Neuroscience and Clinical Research." *NeuroImage* 194: 191–210. <https://doi.org/10.1016/j.neuroimage.2019.01.029>.
- Tardif, C. L., C. J. Gauthier, C. J. Steele, et al. 2016. "Advanced MRI Techniques to Improve Our Understanding of Experience-Induced Neuroplasticity." *NeuroImage* 131: 55–72. <https://doi.org/10.1016/j.neuroimage.2015.08.047>.
- Taubert, M., B. Draganski, A. Anwander, et al. 2010. "Dynamic Properties of Human Brain Structure: Learning-Related Changes in Cortical Areas and Associated Fiber Connections." *Journal of Neuroscience* 30: 11670–11677. <https://doi.org/10.1523/JNEUROSCI.2567-10.2010>.
- Taubert, M., G. Lohmann, D. S. Margulies, A. Villringer, and P. Ragert. 2011. "Long-Term Effects of Motor Training on Resting-State Networks

- and Underlying Brain Structure.” *NeuroImage* 57: 1492–1498. <https://doi.org/10.1016/j.neuroimage.2011.05.078>.
- Taubert, M., J. Mehnert, B. Pleger, and A. Villringer. 2016. “Rapid and Specific Gray Matter Changes in M1 Induced by Balance Training.” *NeuroImage* 133: 399–407. <https://doi.org/10.1016/j.neuroimage.2016.03.017>.
- Taubert, M., E. Roggenhofer, L. Melie-Garcia, et al. 2020. “Converging Patterns of Aging-Associated Brain Volume Loss and Tissue Microstructure Differences.” *Neurobiology of Aging* 88: 108–118. <https://doi.org/10.1016/j.neurobiolaging.2020.01.006>.
- Thomas, C., and C. I. Baker. 2013. “Teaching an Adult Brain New Tricks: A Critical Review of Evidence for Training-Dependent Structural Plasticity in Humans.” *NeuroImage* 73: 225–236. <https://doi.org/10.1016/j.neuroimage.2012.03.069>.
- Todorich, B., J. M. Pasquini, C. I. Garcia, P. M. Paez, and J. R. Connor. 2009. “Oligodendrocytes and Myelination: The Role of Iron.” *Glia* 57: 467–478. <https://doi.org/10.1002/glia.20784>.
- Tofts, P. 2003. *Quantitative MRI of the Brain: Measuring Changes Caused by Disease*. Vol. xvi, 633. Wiley, Chichester West Sussex: Hoboken NJ.
- Tran, P. V., B. C. Kennedy, Y.-C. Lien, R. A. Simmons, and M. K. Georgieff. 2015. “Fetal Iron Deficiency Induces Chromatin Remodeling at the Bdnf Locus in Adult Rat hippocampus. American Journal of Physiology.” *Regulatory, Integrative and Comparative Physiology* 308: R276–R282. <https://doi.org/10.1152/ajpregu.00429.2014>.
- Trefler, A., N. Sadeghi, A. G. Thomas, C. Pierpaoli, C. I. Baker, and C. Thomas. 2016. “Impact of Time-Of-Day on Brain Morphometric Measures Derived From T1-Weighted Magnetic Resonance Imaging.” *NeuroImage* 133: 41–52. <https://doi.org/10.1016/j.neuroimage.2016.02.034>.
- Turati, L., M. Moscatelli, A. Mastropietro, et al. 2015. “In Vivo Quantitative Magnetization Transfer Imaging Correlates With Histology During de- and Remyelination in Cuprizone-Treated Mice.” *NMR in Biomedicine* 28: 327–337. <https://doi.org/10.1002/nbm.3253>.
- Tymofiyeva, O., and R. Gaschler. 2020. “Training-Induced Neural Plasticity in Youth: A Systematic Review of Structural and Functional MRI Studies.” *Frontiers in Human Neuroscience* 14: 497245. <https://doi.org/10.3389/fnhum.2020.497245>.
- Weber, A. M., Y. Zhang, C. Kames, and A. Rauscher. 2020. “Myelin Water Imaging and R2* Mapping in Neonates: Investigating R2* Dependence on Myelin and Fibre Orientation in Whole Brain White Matter.” *NMR in Biomedicine* 33: e4222. <https://doi.org/10.1002/nbm.4222>.
- Weiskopf, N., S. Mohammadi, A. Lutti, and M. F. Callaghan. 2015. “Advances in MRI-Based Computational Neuroanatomy: From Morphometry to In-Vivo Histology.” *Current Opinion in Neurology* 28: 313–322. <https://doi.org/10.1097/WCO.0000000000000222>.
- Weiskopf, N., J. Suckling, G. Williams, et al. 2013. “Quantitative Multi-Parameter Mapping of R1, PD(*), MT, and R2(*) At 3T: A Multi-Center Validation.” *Frontiers in Neuroscience* 7: 95. <https://doi.org/10.3389/fnins.2013.00095>.
- Wenger, E., C. Brozzoli, U. Lindenberger, and M. Lövdén. 2017. “Expansion and Renormalization of Human Brain Structure During Skill Acquisition.” *Trends in Cognitive Sciences* 21: 930–939. <https://doi.org/10.1016/j.tics.2017.09.008>.
- Wenger, E., S. Kühn, J. Verrel, et al. 2017. “Repeated Structural Imaging Reveals Nonlinear Progression of Experience-Dependent Volume Changes in Human Motor Cortex.” *Cerebral Cortex* 27: 2911–2925. <https://doi.org/10.1093/cercor/bhw141>.
- Wenger, E., S. E. Polk, M. M. Kleemeyer, et al. 2022. “Reliability of Quantitative Multiparameter Maps Is High for Magnetization Transfer and Proton Density but Attenuated for R1 and R2 * in Healthy Young Adults.” *Human Brain Mapping* 43: 3585–3603. <https://doi.org/10.1002/hbm.25870>.
- Winkler, A. M., G. R. Ridgway, M. A. Webster, S. M. Smith, and T. E. Nichols. 2014. “Permutation Inference for the General Linear Model.” *NeuroImage* 92: 381–397. <https://doi.org/10.1016/j.neuroimage.2014.01.060>.
- Winkler, A. M., M. A. Webster, J. C. Brooks, I. Tracey, S. M. Smith, and T. E. Nichols. 2016. “Non-Parametric Combination and Related Permutation Tests for Neuroimaging.” *Human Brain Mapping* 37: 1486–1511. <https://doi.org/10.1002/hbm.23115>.
- Wonderlick, J. S., D. A. Ziegler, P. Hosseini-Varnamkhasti, et al. 2009. “Reliability of MRI-Derived Cortical and Subcortical Morphometric Measures: Effects of Pulse Sequence, Voxel Geometry, and Parallel Imaging.” *NeuroImage* 44: 1324–1333. <https://doi.org/10.1016/j.neuroimage.2008.10.037>.
- Yasuda, M., E. M. Johnson-Venkatesh, H. Zhang, J. M. Parent, M. A. Sutton, and H. Umemori. 2011. “Multiple Forms of Activity-Dependent Competition Refine Hippocampal Circuits In Vivo.” *Neuron* 70: 1128–1142. <https://doi.org/10.1016/j.neuron.2011.04.027>.
- Yeatman, J. D., B. A. Wandell, and A. A. Mezer. 2014. “Lifespan Maturation and Degeneration of Human Brain White Matter.” *Nature Communications* 5: 4932. <https://doi.org/10.1038/ncomms5932>.
- Zatorre, R. J., R. D. Fields, and H. Johansen-Berg. 2012. “Plasticity in Gray and White: Neuroimaging Changes in Brain Structure During Learning.” *Nature Neuroscience* 15: 528–536. <https://doi.org/10.1038/nn.3045>.
- Ziminski, J. J., P. Frangou, V. M. Karlaftis, U. Emir, and Z. Kourtzi. 2023. “Microstructural and Neurochemical Plasticity Mechanisms Interact to Enhance Human Perceptual Decision-Making.” *PLOS Biology* 21: e3002029. <https://doi.org/10.1371/journal.pbio.3002029>.

Supporting Information

Additional supporting information can be found online in the Supporting Information section.